Effect of the pion and Δ optical potential on deep inelastic pion-nuclear reactions

Joseph N. Ginocchio and Mikkel B. Johnson
Los Alamos Scientific Laboratory, Los Alamos, New Mexico 87544
(Received 17 April 1979)

The effect of the pion and Δ optical potentials on the propagation of the pion and delta in a semiclassical transport model of pion-nuclear reactions is studied. It is shown that the reaction and true absorption cross sections are increased to become closer to the measured cross sections. The derivative terms in the optical potential are shown to be particularly important. However, the distribution of final products produced still has some discrepancies compared to experiment, indicating that the mechanism for the deposition of the pion energy in the nucleus is not completely understood.

[NUCLEAR REACTIONS The effect of optical potential on mean free paths in pion-nucleus reactions. Total reaction and absorption cross section calculated for pions incident on ^{12}C.]

The intranuclear cascade model[1-3] has been very useful in calculating pion and nucleon spectra and spallation cross sections for nucleon- and pion-induced reactions. This model is a classical transport model and therefore, in order to calculate these complicated reactions as accurately as possible, it is necessary that the propagation of the incoming particle through the nucleus be as correct as possible. Recent calculations[1] of pion total reaction cross section and true absorption cross sections using the intranuclear cascade model have underestimated these cross sections, particularly below the pion (3-3) resonance energy. The total reaction cross section depends importantly on the delta mean free path. In these calculations[1,3] the effect of the pion optical potential on the propagation of the pion has been ignored. The average pion mean free path in these calculations is

$$\lambda_0^{-1}=\bar{\sigma}\rho(r)\,. \tag{1a}$$

Here $\rho(r)$ is the total nuclear density and

$$\bar{\sigma}=\frac{N}{A}\sigma_n+\frac{Z}{A}\sigma_p\,, \tag{1b}$$

where σ_n and σ_p are the total pion-neutron and pion-proton cross sections, and N, Z, and A are the neutron, proton, and nucleon numbers for the target. In this paper we would like to explore the effects of the optical model on the propagation of the pion in the intranuclear cascade model. We will do this by using the mean free path derived for a pion influenced by an optical potential U. We will also study true pion absorption by looking at alternative delta absorption mechanisms.

In nuclear matter the wave function of the pion $\psi(r)$ satisfies the Klein-Gordon equation

$$[-\nabla^2+U(r)]\psi(r)=k^2\psi(r)\,, \tag{2}$$

where

$$k^2=(E-V_c)^2-\mu^2 \tag{3}$$

and E is the total incident pion energy, V_c is the pion-nuclear Coulomb energy, and μ is the pion mass. The simple first-order optical potential in which the free pion-nucleon scattering amplitude is used is inadequate for describing pion-nucleus interactions. This has been known both from pionic atom studies[4] and from attempts to fit elastic pion-nucleus scattering experiments throughout the region of the (3-3) resonance.[5-7] An expression for the optical potential including the most important corrections takes the form

$$U(r)=-b_0k^2\rho(r)+b_1\nabla\left[\rho(r)\Big/\left(1+\frac{\xi b_1}{3}\rho(r)\right)\right]\nabla - 4\pi B_0\rho^2(r)+\text{Pauli} + \text{resonance-broadening effects}\,. \tag{4}$$

Here b_0 and b_1 are related to the free s- and p-wave pion-nucleon scattering amplitude in the usual way,[5] and are evaluated at the pion laboratory momentum k. B_0 is a parameter describing s-wave true pion absorption[8] and has the value $B_0=0.168\,(-1+i)$ fm^4. The quantity ξ is the Lorentz-Lorenz parameter and depends on the short-range nucleon-nucleon correlations.[9] Estimates of ξ range from 0 to 1.2. The long-range Pauli correlation is included in a separate term, as is the broadening[7,10,11] of the (3-3) resonance. Resonance broadening includes effects of true pion absorption and multiple reflections of the pion among the nucleons of the nucleus.

In order to make use of these results in the intranuclear cascade model, it is necessary to make a semiclassical approximation to Eq. (2). This

may be accomplished as follows. The form of the Klein-Gordon equation is

$$-\nabla^2\psi - \nabla\cdot\alpha\nabla\psi + \beta\psi = k^2\psi\,, \tag{5}$$

where $\alpha(r)$ and $\beta(r)$ will be specified for the specific models below. To identify the pion wave number, it is useful to make the transformation from ψ to χ,[4] where

$$\psi(r) = \chi(r)/[1+\alpha(r)]^{1/2}\,. \tag{6}$$

The equation for χ takes the form

$$-\nabla^2\chi + \tilde{U}(r)\chi = k^2\chi\,, \tag{7}$$

where

$$\tilde{U}(r) = \frac{1}{2}\frac{\nabla^2\alpha}{1+\alpha} - \frac{(\frac{1}{2}\alpha')^2}{(1+\alpha)^2} + \frac{\alpha k^2}{1+\alpha} + \frac{\beta}{1+\alpha}\,. \tag{8}$$

The potential in Eq. (7) is *local* and hence a semiclassical description of χ is possible. The local wave number $K(r)$ is given by

$$K^2(r) = k^2 - \tilde{U}(r)\,. \tag{9}$$

In uniform nuclear matter the derivative terms in Eq. (8) drop out and the result for K, and hence for the mean free path λ, is the same as one would obtain from a nuclear matter calculation through the pion Green's function (see, for example, Ref. 11). In the nuclear surface, there are additional terms in Eq. (9) which arise from the nonlocal character of the interaction in Eq. (5). These gradient terms are known to be important; they have been discussed in Ref. 4 in the context of pionic atom physics and in Ref. 12 in the context of pion scattering.

In the semiclassical approximation, the wave function χ is given by

$$\chi(r) = C\exp\left(i\int_{-\infty}^{z}[K(x,y,z') - k]\,dz'\right) \tag{10}$$

and hence $\psi(r)$, from Eq. (6), by

$$\psi(r) = C\exp\left(i\int_{-\infty}^{z}[K(x,y,z') - k]\,dz' - \tfrac{1}{2}\ln[1+\alpha(r)]\right)$$

$$= C\exp\left\{i\int_{-\infty}^{z}\left[K(x,y,z') - k + \frac{i}{2}\frac{\partial'_z\alpha(x,y,z')}{1+\alpha(r)}\right]dz'\right\}. \tag{11}$$

In this approximation, the probability that the pion will be found at a distance r in the nucleus is $|\psi(r)|^2$, where from Eq. (11)

$$|\psi(r)|^2 = |C|^2\exp\left\{-2\left[\int_{-\infty}^{z}\mathrm{Im}K(x,y,z') + \tfrac{1}{2}\mathrm{Re}\left(\frac{1}{1+\alpha(r)}\frac{d}{dz'}\times\alpha(x,y,z')\right)dz'\right]\right\}.$$

We thus identify the pion mean free path λ along the direction $\hat{k}$ as

$$\lambda = \frac{1}{2\left[\mathrm{Im}K(r) + \frac{\hat{k}}{2}\cdot\mathrm{Re}\left(\frac{\nabla\alpha}{1+\alpha}\right)\right]}\,. \tag{12}$$

In this work we shall ignore the second term in the denominator of Eq. (12) because it vanishes along the circumference of the nucleus ($z=0$) and should therefore have essentially no effect on the total cross sections. The term, furthermore, vanishes inside the nucleus, where ρ = constant. In the limit of ρ small, that is,

$$\rho\,|b_0 + b_1| \ll 1\,, \tag{13}$$

and constant as a function of position, the mean free path λ will become equal to λ_0, which is defined in Eq. (1).

In addition to specifying the dynamics of the pion, we must also specify the dynamics of the delta in the intranuclear cascade model. The delta dynamics are closely related to the "true absorption" of the pion, which takes place in two steps. In the first step a delta, Δ, is formed in pion-nucleon resonant scattering. The delta then propagates as a particle and then decays,

$$\Delta \to \pi + N\,, \tag{14a}$$

or collides with another nucleon and goes into two nucleons, that is,

$$\Delta + N \to N_1 + N_2\,. \tag{14b}$$

This we refer to as the delta absorption mechanism; it leads to the absorption of the pion. In Ref. 1 this cross section was calculated in a one-pion exchange model with a form factor with one range parameter. This range parameter was determined by fitting the pion production cross section for the scattering of 1-GeV protons from a free proton at rest,[13] which is the inverse of the reaction given in Eq. (14):

$$N_1 + N_2 \to \Delta + N_2' \to N_1' + N_2' + \pi\,. \tag{15}$$

As can be seen by the dashed line in Fig. 1, this choice underestimates the pion production at lower

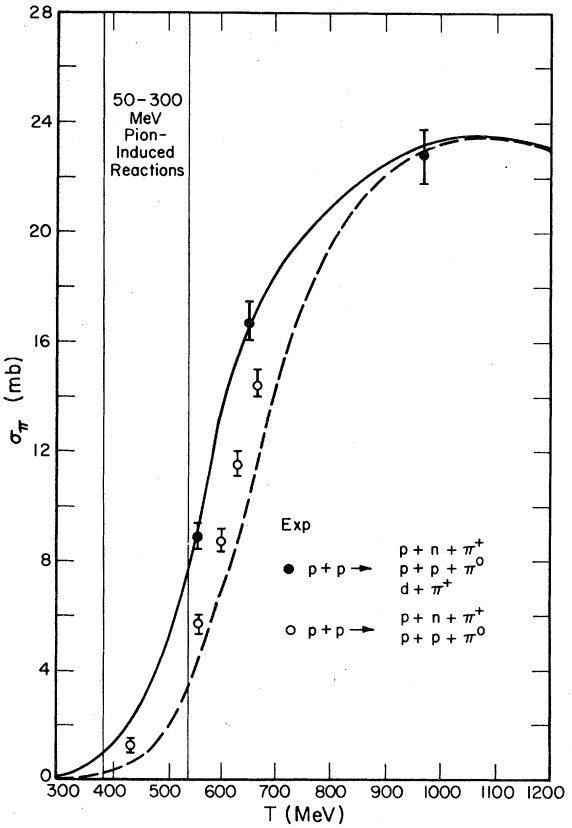

FIG. 1. The experimental and calculated pion production cross section σ_π for protons with kinetic energy T incident on a proton target. The circles are the measured experimental data taken from Ref. 13. The full circles include $p+p \rightarrow d+\pi^+$, whereas the open circles do not. The dashed curve represents the calculation of pion production from the model of Ref. 1. The solid curve is a fit to the data by multiplying the results of the dashed curve by a factor dependent on the kinetic energy T. True absorption in pion-induced reactions in the resonance region depends on the pion production cross section between the two vertical lines.

energies. In particular, for pions incident with energies in the resonance region, the delta absorption cross section corresponds to pion production for nucleons with incident kinetic energies ranging from 400 to 500 MeV, as illustrated in Fig. 1. The pion production in this energy range is badly underestimated by the delta cross section of Ref. 1, perhaps by as much as a factor of 3. For this reason we have multiplied the delta cross section of Ref. 1 by a factor which depends only on the invariant energy of the delta-nucleon system, i.e., on the kinetic energy of the incident nucleon beam in the reaction of Eq. (15), so as to fit the pion production cross section for low incident nucleon kinetic energies as well. This fit is given by the solid line in Fig. 1.

In this paper we shall examine the effect of the various terms in Eqs. (4) and (8) in two models. The first (Model I) follows closely the philosophy of Ref. 5b in that the resonance-broadening term is dropped in Eq. (4). We examine the sensitivity of the results to ξ; the value $\xi=0$ corresponds to the first-order Kisslinger potential. We also evaluate this model assuming that the derivative terms in Eq. (8) are dropped to show the importance of these. In Model I we use the improved delta-nucleon cross section discussed above in connection with Fig. 1. Explicit forms for α and β in Model I are

$$\alpha = -b_1\rho(r)/[1+\tfrac{1}{3}(\xi b_1)\rho(r)]\,,$$
$$\beta = -b_0k^2\rho(r) - 4\pi B_0\rho^2(r)\,. \tag{16}$$

Model II follows more closely the philosophy of Ref. 7; that is, we keep the resonance-broadening term and set $\xi=0$. The values for α and β are

$$\alpha = -b_1'\rho(r)\,,\quad \beta = -b_0k^2\rho(r)\,, \tag{17}$$

where b_1' is given by

$$b_1' = b_1\left[\frac{E-E_R+\frac{1}{2}(i\Gamma)}{E-E_R+\frac{1}{2}(i\Gamma)-W(E)\rho(r)/\rho(0)}\right], \tag{18}$$

where E is the pion laboratory kinetic energy, E_R and Γ are the (3-3) resonance energy and width, respectively, and where $W(E)$ is the isobar-spreading interaction taken from the fit of Hirata *et al.*[7c] to elastic scattering from ^{16}O. The $W(E)$ has a real and an imaginary part which depend strongly on energy. We have parametrized the results of Ref. 7c and found the following representation of the spreading interaction:

$$W(E) = (98.5+14.4i) - (1.18+0.805i)E + (0.003+0.0023i)E^2\,,$$
$$50 \leq E-\mu \leq 300 \text{ MeV},\quad W \text{ in MeV}. \tag{19}$$

The potential $W(E)$ may be regarded as the single particle potential experienced by the (3-3) resonance. The real part of $W(E)$ includes the effect of the binding of the nucleons. The imaginary part of $W(E)$ arises from collision broadening (including pion "multiple reflections") and from true absorption of the pion. We shall assume that all resonance-broadening mechanisms ultimately lead to the pion's being absorbed. This assumption is the basis for our delta absorption mechanism in Model II, which takes the delta mean free path for absorption directly from the imaginary part of Eq. (19). The relation between the Δ mean absorption free path and $W(E)$ is

$$\lambda_{\text{abs}} = \frac{197\rho(0)}{2\,\text{Im}\,W(E)\rho(r)}. \tag{20}$$

In the intranuclear cascade model a microscopic calculation of the pion propagation through the nucleus is done using a Monte Carlo technique. The Pauli principle is taken into account approximately by allowing only those collisions in which a nucleon after a collision has a momentum greater than the Fermi momentum. In any particular collision, the probability $P_i(x)$ that a collision between the pion and a nucleon of type i (neutron or proton) takes place within a distance x from some point, must be specified. This probability is taken to be

$$P_i(x) = (1 - e^{-x/\lambda}) p_i , \tag{21a}$$

where the factor $1 - e^{-x/\lambda}$ specifies the probability that the pion will be scattered in the distance x and p_i is the probability of interacting with i. The quantity λ is the pion mean free path; it is the sensitivity of the results of the intranuclear cascade model to this quantity which we are examining in this paper. Because the Pauli principle is taken into account in the manner stated above, we have dropped the Pauli term in Eq. (4) to avoid possible double counting. Thus, the λ evaluated in Models I and II contains no explicit Pauli suppression effect. The validity of this treatment deserves further study. We take

$$\rho_i = \frac{\sigma_i \rho_i}{\bar{\sigma} \rho} , \tag{21b}$$

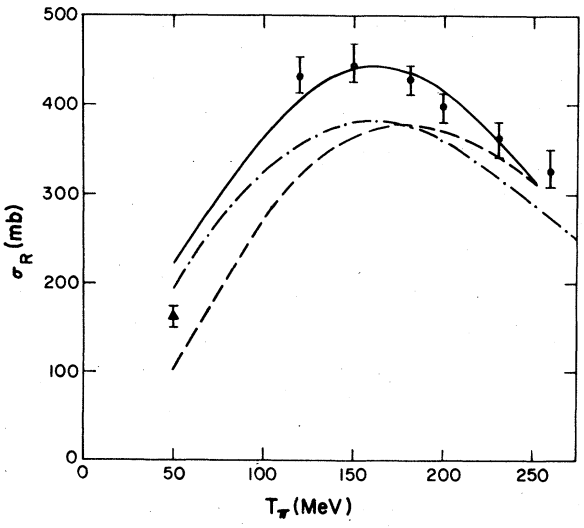

FIG. 2. The total reaction cross section σ_R for negative pions incident on ^{12}C as a function of the pion kinetic energy T_π. The full circles with error flags are the measured values from Ref. 14. The full triangle is a measurement on ^{12}C from Ref. 23. The dashed line is the calculation of Ref. 1, i.e., no optical model refinements of the pion mean free path. The solid curve is the calculation in Model I for $\xi = 0$. When the gradient terms in Eq. (8) are dropped, the result is the dot-dashed curve.

where ρ_i is the partial density of nucleon species i, where $\bar{\sigma}$, σ_i, and ρ are defined below Eq. (1), where $\bar{\sigma}$ and λ are evaluated at the pion laboratory energy [see Eq. (3)], and where σ_i is evaluated at the pion-nucleon center-of-mass energy. It would be better to use p_i calculated in the medium rather than free space cross sections; we have assumed that the medium corrections are less important in the ratio in Eq. (10b) than they are in the individual σ_i and $\bar{\sigma}$. Similar considerations apply to the dynamics of the Δ and nucleon.

In Fig. 2 the total measured reaction cross section[14] for negative pions incident on ^{12}C is compared to the calculated values. The dashed line corresponds to the calculation with no optical model refinements, i.e., λ given in Eq. (1). Note that this calculation underestimates the cross section for all but the highest energies, and appears to peak at too high an energy. The calculation in Model I, $\xi = 0$, gives the solid curve. Note that the magnitude of the reaction cross section is now in much better agreement with the data and that the peak has shifted to lower energies. To see the importance of the derivative terms, we have also made a calculation in which these are not included (the dot-dash curve). These have their largest effect on the reaction cross section in the vicinity of the (3-3) resonance. The nonderivative corrections to the optical potential have their largest effect at low energy and relatively small effect at resonance.

In Fig. 3 we show the reaction cross section again. The dashed curve is the same as in Fig. 2. The solid curve is Model I, $\xi = 1.2$. The Lorentz-

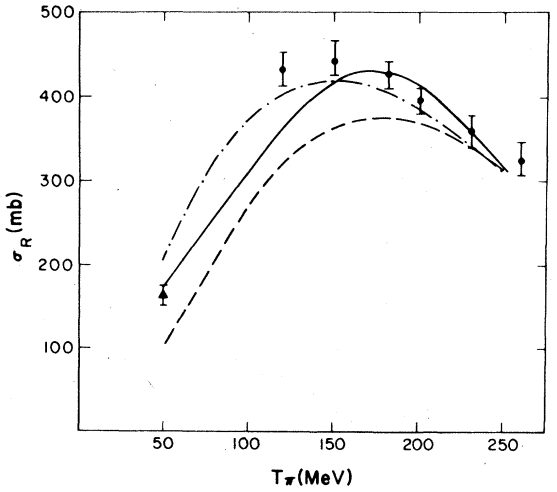

FIG. 3. The total reaction cross section σ_R for negative pions incident on ^{12}C as a function of the pion kinetic energy T_π. The data and dashed curve are the same as in Fig. 2. The solid curve is Model I, $\xi = 1.2$. The dot-dashed curve is Model II.

Lorenz effect is well known to weaken the optical potential at high density and this is reflected in the calculation. Note that the largest effect occurs at low energy; this is to be expected, as the nucleus is more transparent and the pion is more able to be influenced by the high-density region of the nucleus. The effect is rather dramatic, substantially underestimating the σ_R and shifting the peak to higher energies in disagreement with the data. Also shown in the figure is the calculation of Model II. This result is surprisingly similar to Model I, $\xi = 0$. The reason is that at low energy the shift of the resonance due to $W(E)$ (upward) results in a decreasing of the imaginary part of the optical potential, which is compensated by a broadening of the resonance. The largest effect is found in the resonance region, and the effect is to *decrease* the reaction cross section so that the data are slightly underestimated.

All three optical potentials, Model I with $\xi = 0$ and $\xi = 1.2$, and Model II with $\xi = 0$, reproduce the reaction cross section near the resonance, and are an improvement over the intranuclear cascade calculated without the optical potential. Also, all three optical models give reasonable fit to the elastic scattering since it is primarily diffractive at that energy. As the energy is decreased, the elastic scattering is reproduced better by Model I, $\xi = 1.2$, and Model II. Model II seems to better fit the Binon data[14] through the resonance. However, Model I with $\xi = 1.2$ seems to fit the low-energy reaction cross section. (We evaluated this point by using the phase-shift analysis A in Ref. 23. This point does not seem to be unambiguously determined by the elastic scattering.)

We have only crudely accounted for the finite range of the pion-nucleon interaction in our calculation. In Ref. 15 it is shown that the finite range may be approximately compensated by adjusting the nuclear radius so that the new rms radius R' is related to the actual nuclear rms radius R_N of point nucleons by

$$R'^2 = R_N^2 + R_{\pi N}^2 , \tag{22}$$

where $R_{\pi N}$ is the rms radius of the pion-nucleon interaction. Estimates[15] of $R_{\pi N}$ vary from ~1.36 fm in Ref. 16 to ~0.38 fm in Ref. 17. In our work we have used for R' the nuclear charge radius, which differs from the radius for point nucleons by approximately

$$R'^2 = R_N^2 + (0.8 \text{ fm})^2 . \tag{23}$$

0.8 fm is the charge radius of the proton. A crude estimate of the dependence of the error $\Delta\sigma_R$ in σ_R on the radius of the pion-nucleon interaction is given by[15]

$$\Delta\sigma_R = \tfrac{2}{3}\Delta(\pi R'^2) . \tag{24}$$

For the two extremes of $R_{\pi N}$ (1.34 vs 0.38 fm), we get

$$\Delta\sigma_R = \begin{cases} +24 \text{ mb for } R_{\pi N} = 1.34 \text{ fm} \\ -10 \text{ mb for } R_{\pi N} = 0.38 \text{ fm} . \end{cases} \tag{25}$$

The true absorption cross section calculated with the model of Ref. 1 for positive pions incident on ^{12}C as a function of pion energy is compared to the measured cross sections[18] in Fig. 4. The solid triangles are derived from measurements[18b] on ^{16}O by multiplying the cross sections by a factor $(\frac{12}{16})^{0.77} \simeq 0.8$ to take into account the smaller size of carbon.[1] The dashed curve is the calculation for the delta absorption cross section from Ref. 1 while the points are the measured cross sections. In Ref. 1 these calculated cross sections were compared to bubble-chamber measurements of the pion absorption cross section. However, with the exception of Ref. 18a, it is unclear to what extent the production of π^0 was accounted for in these experiments. For this reason, and because other pion absorption data is becoming available, these data are omitted from Fig. 4. The calculated cross section underestimates the measured cross section at low energies and overestimates it at high energies.

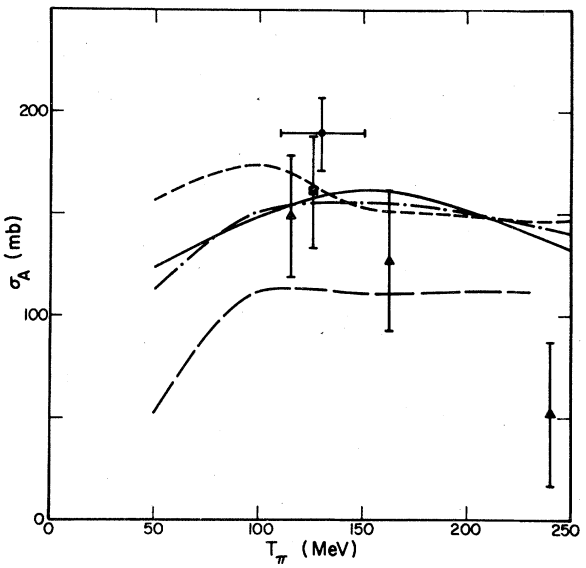

FIG. 4. The true pion absorption cross section σ_A for positive pions incident on ^{12}C as a function of pion kinetic energy T_π. The dashed line corresponds to the delta absorption model of Ref. 1. The solid line is Model I, $\xi = 1.2$, the dashed line is Model I, $\xi = 0$, and the dot-dashed line is Model II. The solid circle is from Ref. 18a, the solid triangles from Ref. 18b, and the solid square from Ref. 18c.

In Fig. 5 the calculated percentage for pion absorption is compared to the measured values and these agree for the two lower energies, but overestimate at the high energy. However, the error bars are very large on the experimental cross sections. The dashed curve in Fig. 5 is calculated in the same model as the dashed curve in Fig. 4.

Using the new delta absorption cross section of Model I, we get a very substantial improvement in the magnitude of the true pion absorption cross section at low energies, as seen by the solid and short dashed lines in Fig. 4. In these cases the pion mean free path was calculated from Model I. The short dashed curve corresponds to $\xi = 0$ and the solid curve to $\xi = 1.2$. Hence, by using a delta absorption cross section which fits the pion production cross section, we can nearly reproduce the true pion absorption in finite nuclei for energies below the resonance. This also tells us that the one-pion exchange model with a form factor is inadequate for both pion production and pion absorption.

The magnitude of the cross section for the delta absorption reaction, Eq. (14), is determined from a measurement for pion production made in *free* space. This scattering amplitude in the nucleus could be altered just as the pion scattering amplitude is changed inside the nucleus. For this reason, theoretical study of the Δ optical potential should be pursued. The dot-dashed curves in Figs. 4 and 5 show the calculation of the absolute and relative absorption cross sections in Model II. We see a near agreement in both the magnitude of the absorption cross section and the percentage absorption to total reaction cross section compared to the measured values for low-energy incident pions. However, a discrepancy remains for pions with energy above 150 MeV. This may mean that it is incorrect to identify the spreading interaction W entirely with true absorption, as we have done.

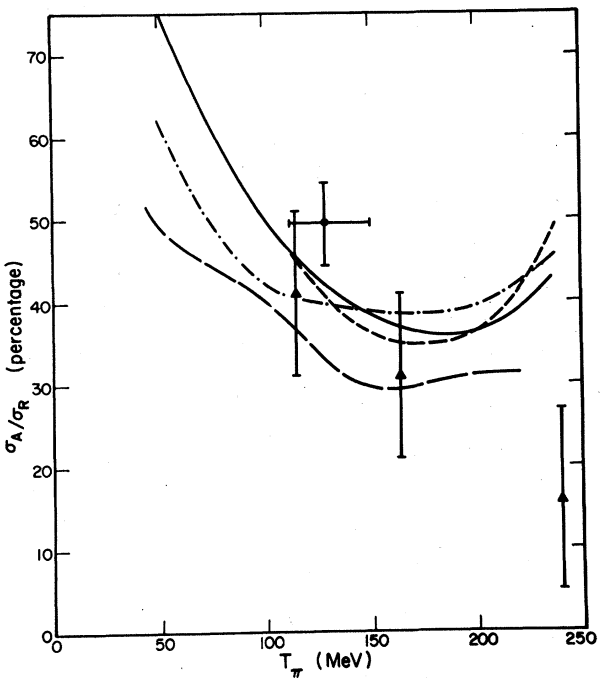

FIG. 5. The ratio of the true pion absorption cross section for positive pions incident on ^{12}C as a function of pion kinetic energy T_π. The legend is the same as in Fig. 4.

The bubble-chamber data is rather crude, but there do exist other indirect measures of true pion absorption. For example, the measurement of the high-energy proton spectra from pion-induced reactions provide a good measure of true pion absorption.[19] The energy dependence of the differential cross section is given quite well by the intranuclear cascade model.[1] However, the magnitudes are underestimated at forward angles, especially in the case of 100-MeV incident positive pions. In Table I we show the experimental cross section $d\sigma/d\Omega$ for 100-MeV incident π^+ on ^{27}Al, where

$$d\sigma/d\Omega = \int_{E_p=60\ \mathrm{MeV}}^{\infty} dE_p \frac{d\sigma^2}{d\Omega dE_p},$$

and theoretical calculations of the same quantity at 45° and 94°. The calculation employed was Model I with the improved model of pion absorption. The column "Ref. 1" shows the previous discrepancy at forward angles. Inclusion of the optical potential improves the magnitude of the cross section; the calculation is still more isotropic than the experiment. However, the sum of the measured cross sections at the two angles is 56 ± 9 mb/sr, in good agreement with the calculated sum of 45–55 mb/sr. Perhaps the angular distribution used for the delta absorption mechanism is not correct.

Although the inclusion of the pion optical potential and the larger delta-nucleon cross section have

TABLE I. 100-MeV π^+ on ^{27}Al differential proton spectrum for $E_p \geq 60$ MeV. The differential cross section for producing protons with energy $E_p > 60$ MeV for incident positive pions is tabulated for two angles, $\theta = 45°$ and 94°. The entries in the table are the measured values (Ref. 19) (Exp), the calculated values from Ref. 1, and the calculated values with Model I for two values of the Lorentz-Lorenz Ericson-Ericson parameter ξ.

	$\frac{d\sigma}{d\Omega}$ (mb/sr)			
θ	Exp	Ref. 1	Model I ($\xi = 0$)	Model I ($\xi = 1.2$)
45°	39 ± 8	18 ± 1	30 ± 2	25 ± 2
94°	17 ± 2	14 ± 1	23 ± 2	20 ± 2

improved the total pion reaction and absorption cross section, the deposition of the energy in this semiclassical model has some difficulties. Two puzzles still remain. One of them is the nucleon knockout cross sections. The intranuclear cascade predicts approximately the correct nucleon knockout cross sections for heavy nuclei, through the resonance region, but not for light nuclei.[20,21] This discrepancy remains, even with the improved pion optical potential.

The other puzzle is with respect to the mass distribution of spallation products for pion-induced reactions on nuclei. Recent measurements of spallation products,[22] which combine prompt γ-ray and radioactivity measurements of the residual nuclei, show that there are large cross sections for producing products with four to six nucleons removed from the target which the intranuclear cascade cannot seem to predict. In Fig. 6 the spallation cross section for 200-MeV π^+ incident on ^{62}Ni is shown as a function of ΔA, where

$$\Delta A = 62 - A_p ,$$

and A_p is the mass of the measured spallation products. The solid circles are the measured cross section and the dashed line indicates the trend of the data. The triangles are the calculated cross section for the same products as measured, and the solid line indicates the trend. We exclude the products with $\Delta A < 3$ since there are more uncertainties in these measured cross sections. Whereas the measured spallation cross section goes through a maximum for $\Delta A = 4$, the calculated cross section monotonically decreases tending towards the measured cross section for ΔA large. This discrepancy could imply a more complicated mechanism for the deposition of pion energy than is now present in the intranuclear cascade model.

We have shown in this paper that when pion and Δ optical potentials are used which give reasonable fits to the pion-nucleus elastic scattering, and to nucleon-nucleon pion production data in the case of the delta, the intranuclear cascade model gives total pion reaction and true absorption cross sections in finite nuclei in much better agreement with the measured values. One important result of the calculations presented here is that the total reaction cross section is sensitive to the higher-order terms in the pion optical potential at low energy. This means, among other things, that more reaction cross-section data, especially at the lower energies (below 120 MeV), is desirable and is of fundamental importance in determining the reaction dynamics. Also, better true pion absorption

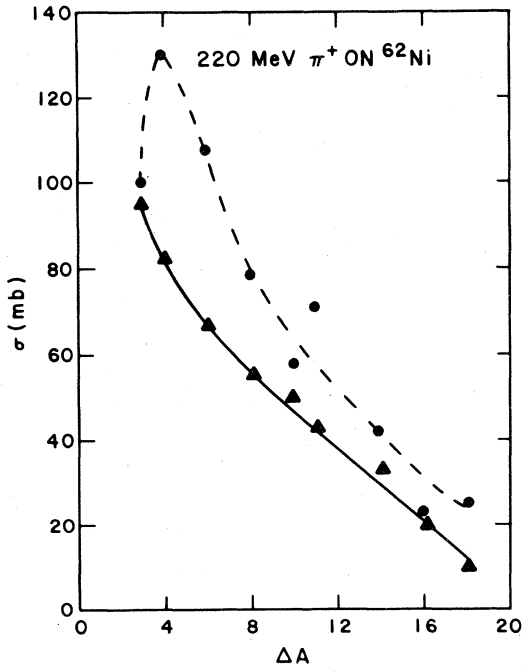

FIG. 6. The spallation cross section σ for 220-MeV positive pions incident on ^{62}Ni as a function of the number of nucleons removed from the target ΔA. The solid circles are the data taken from Ref. 22, and the dashed line indicates the trend in the data. The open triangles are the calculated cross sections for the same isotopes measured and the solid line indicates the trend.

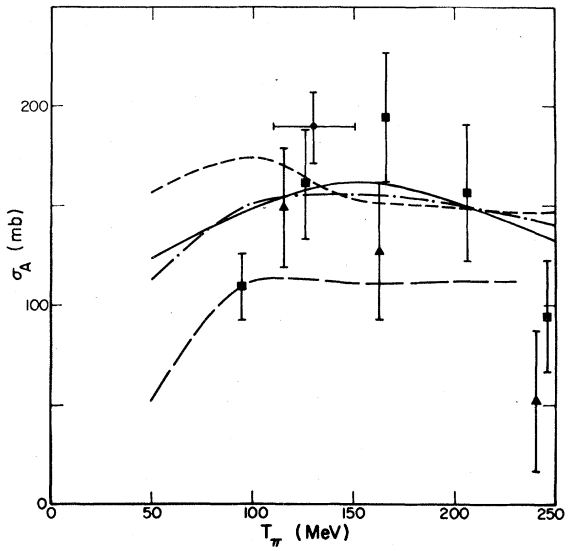

FIG. 7. The true pion absorption cross section σ_A for positive pions incident on ^{12}C as a function of pion kinetic energy T_π. The dashed line corresponds to the delta absorption model of Ref. 1. The solid line is Model I, $\xi = 1.2$, the dotted line is Model I, $\xi = 0$, and the dot-dashed line is Model II. The solid circle is from Ref. 18a, the solid triangles from Ref. 18b, and the solid squares from Ref. 18c and the recent data of Navon *et al.* referred to in the text.

data is needed through the resonance region. The calculated absorption cross section, while agreeing with the measured values at and below the resonance energy, does not fall as fast with energy as the measured absorption cross sections. However, old bubble-chamber measurements[24] give an absorption cross section of 203 ±20 mb at 195 MeV incident π^+. Even though this may be a crude measurement, it is a factor of 2 larger than that implied by the trend in Fig. 4. It will be desirable to determine these cross sections firmly. A number of other puzzles remain. These suggest that at least in certain reactions the dynamics are more complicated than we have anticipated. The intranuclear cascade model is flexible enough to accommodate alternative reaction mechanisms and therefore to serve as a means to further study the underlying physics.

Note added. We have learned of recent measurements of the true pion absorption cross section σ_A for positive pions incident on ^{12}C as a function of incident pion energy by Navon, Ashery, Azuelos, Pfeiffer, Walter, and Schleputz. These measurements give a different impression of the experimental trend than those of Ref. 18b. As seen in Fig. 7, the data of Ref. 18b indicate a falloff of σ_A over the resonance, whereas that of Navon *et al.* show a peak near resonance. The most recent calculations reproduce the average behavior in this energy region. However, these calculations overestimate the absorption at 85 and 250 MeV. Hence, these measured absorption cross sections are more steeply peaked as a function of incident pion energy compared to our most recent calculation.

We wish to thank G. Bertsch for discussions.

[1]J. N. Ginocchio, Phys. Rev. C 17, 195 (1978).
[2]K. Chen, Z. Fraenkel, G. Friedlander, J. R. Grover, J. M. Miller, and Yshimamoto, Phys. Rev. 166, 949 (1968).
[3]G. D. Harp, K. Chen, G. Friedlander, Z. Fraenkel, and J. M. Miller, Phys. Rev. C 8, 581 (1973).
[4]M. Krell and T. E. O. Ericson, Nucl. Phys. B11, 521 (1969).
[5](a) M. Thies, Phys. Lett. 63B, 43 (1976). (b) N. J. Digiacomo, A. S. Rosenthal, E. Rost, and D. A. Sparrow, Phys. Lett. 66B, 421 (1977). (c) G. E. Brown, B. K. Jennings, and V. Rostokin, Phys. Rep. 50, 221 (1979). (d) K. Strikler, H. McManus, and J. A. Carr, C 19, 929 (1979). (e) R. H. Landau and A. W. Thomas, Nucl. Phys. A302, 461 (1978). (f) L. C. Liu and C. M. Shakin, Phys. Rev. C 16, 333 (1977).
[6]L. Kisslinger and W. Wang, Ann. Phys. (N.Y.) 99, 374 (1976).
[7](a) M. Hirata, F. Lenz, and K. Yazaki, Ann. Phys. (N.Y.) 108, 116 (1977). (b) M. Hirata, J. H. Koch, F. Lenz, and E. J. Moniz, Phys. Lett. 70B, 281 (1977). (c) M. Hirata, J. H. Koch, F. Lenz, and E. J. Moniz (unpublished).
[8]J. Hüfner, Phys. Rev. C 21, 1 (1975).
[9]G. Baym and G. E. Brown, Nucl. Phys. A247, 395 (1975).
[10]E. Oset and W. Weise, Phys. Lett. 77B, 159 (1978); E. Oset and W. Weise, Nucl. Phys. A329, 365 (1979).
[11]M. B. Johnson and H. A. Bethe, Nucl. Phys. A305, 418 (1978); and M. B. Johnson and B. D. Keister, *ibid.* A305, 461 (1978).
[12]M. B. Johnson and H. A. Bethe, Comments Nucl. Part. Phys. 8, 75 (1978).
[13]B. S. Neganov and O. V. Savchenko, Zh. Eksp. Teor. Fiz. 32, 1265 (1957) [Sov. Phys.-JETP 5, 1033 (1957)]; Yu. D. Prokoshkin and A. Tiapkin, *ibid.* 32, 750 (1957) [*ibid.* 5, 618 (1957)]; D. V. Bugg, A. J. Oxley, J. A. Zoll, J. G. Rushbrooke, V. E. Barnes, J. B. Kinson, W. P. Dodd, G. A. Doran, and L. Riddiford, Phys. Rev. 133, B1017 (1964); B. Baldoni, S. Focardi, H. Hromadnik, L. Monari, F. Saporetti, S. Femino, F. Mezzanares, E. Bertolini, and G. Gialanella, Nuovo Cimento 26, 1376 (1962); T. H. Fields, J. G. Fox. J. A. Kane, R. A. Stallwood, and R. B. Sutton, Phys. Rev. 109, 1713 (1958); R. A. Stallwood, R. B. Sutton, T. H. Fields, J. G. Fox, and J. A. Kane, *ibid.* 109, 1716 (1958); and V. M. Guzhavin, G. K. Kliger, V. Z. Kolganov, A. V. Lebedev, K. S. Marish, Yu. D. D. Prokoshkin, V. T. Smolyankin, A. P. Sokolov, L. M. Soroko, and T. Wa-Chuang, Zh. Eksp. Teor. Fiz. 46, 1245 (1964) [Sov. Phys.-JETP 19, 847 (1964)].
[14]F. B. Binon, P. Duteil, G. P. Garron, J. Gorres, L. Hugon, J. P. Peigneux, C. Schmit, M. Spighel, and J. P. Stroot, Nucl. Phys. B17, 168 (1970).
[15]M. B. Johnson and D. J. Ernst, Phys. Rev. C 20, 1064 (1979).
[16]J. T. Longergan, K. W. McVoy, and E. J. Moniz, Ann. Phys. (N.Y.) 86, 147 (1974).
[17]D. J. Ernst and M. B. Johnson, Phys. Rev. C 17, 247 (1978); and (unpublished).
[18](a) E. Bellotti, D. Cavalli, and C. Matteuzzi, Nuovo Cimento 18A, 75 (1973). (b) Q. Ingram, J. Bolger, G. Pröbstle, J. Zichy, J. Arvieux, P. Gram, and R. Mischke (unpublished). (c) I. Navon, D. Ashery, G. Azuelos, H. J. Pfeiffer, H. K. Walter, and F. W. Schlepütz (unpublished).
[19]H. E. Jackson, S. B. Kaufman, L. Meyer-Schützmeister, J. P. Schiffer, S. L. Tabor, S. E. Vigdor, J. N. Worthington, L. L. Rutledge, R. E. Segal, R. L. Burman, P. A. M. Gram, R. P. Redwine, and M. A. Yates, Phys. Rev. C 16, 730 (1977).
[20]R. R. Silbar, J. N. Ginocchio, and M. M. Sternheim, Phys. Rev. C 18, 2785 (1978).
[21]S. B. Kaufman, E. P. Steinberg, and G. W. Butler, Phys. Rev. C 20, 262 (1979).
[22]H. E. Jackson, S. B. Kaufman, D. G. Kovar, L. Meyer-Schützmeister, K. E. Rehm, J. P. Schiffer, S. L. Tabor, S. E. Vigdor, T. P. Wangler, L. Rutledge, R. Se-

gal, R. Burman, P. Gram, R. Redwine, and M. Yates-Williams, Phys. Rev. C 18, 2656 (1978).
[23]M. A. Moinester, R. L. Burman, R. P. Redwine, M. A. Yates-Williams, D. J. Malbrough, C. W. Darden, R. D. Edge, T. Marks, S. H. Dam, B. M. Preedom, F. E. Bertrand, T. P. Cleary, E. E. Gross, C. A. Ludemann, M. Blecher, K. Gotow, D. Jenkins, and F. Milder, Phys. Rev. C 18, 2678 (1978).
[24]N. I. Petrov, V. G. Ivanov, and V. A. Rusakov, Zh. Eksp. Teor. Fiz. 37, 957 (1959) [Sov. Phys.-JETP 10, 682 (1960)].